IOP Publishing Journal of Physics D: Applied Physics
J. Phys. D: Appl. Phys. **47** (2014) 255301 (6pp) doi:10.1088/0022-3727/47/25/255301

Interfacial adhesion between graphene and silicon dioxide by density functional theory with van der Waals corrections

Wei Gao[1], Penghao Xiao[2], Graeme Henkelman[2], Kenneth M Liechti[1] and Rui Huang[1]

[1] Department of Aerospace Engineering and Engineering Mechanics, University of Texas at Austin, Austin, TX 78712, USA
[2] Department of Chemistry and the Institute for Computational and Engineering Sciences, University of Texas at Austin, Austin, TX 78712, USA

E-mail: gaowei@utexas.edu

Received 23 March 2014, revised 17 April 2014
Accepted for publication 28 April 2014
Published 30 May 2014

Abstract

Interfacial adhesion between graphene and a SiO_2 substrate is studied by density functional theory (DFT) with dispersion corrections. The results demonstrate the van der Waals (vdW) interaction as the predominant mechanism at the graphene/SiO_2 interface. It is found that the interaction strength is strongly influenced by changes of the SiO_2 surface structures due to surface reactions with water. The adhesion energy is reduced when the reconstructed SiO_2 surface is hydroxylated, and further reduced when covered by a monolayer of adsorbed water molecules. Moreover, it is noted that vdW forces are required to accurately model the graphene/SiO_2 interface with DFT and that the adhesion energy is underestimated by empirical force fields commonly used in atomistic simulations.

Keywords: graphene, adhesion, silicon dioxide, DFT, van der Waals

(Some figures may appear in colour only in the online journal)

Graphene, a two-dimensional crystal membrane, has drawn tremendous interest due to its remarkable electronic and mechanical properties. With respect to applications such as graphene-based nanoelectronic devices [1], the interfacial properties between graphene and the supporting substrate are of great importance. Interfacial adhesion energies have been measured for graphene on various substrate materials such as silicon dioxide (SiO_2) [2–4] and copper [5, 6]. The SiO_2 substrate was instrumental for the first experimental observation of mechanically exfoliated graphene [7] and has been widely used as a dielectric medium in integrated circuits. Using a combined scanning electron microscopy/atomic force microscopy/scanning tunnelling microscopy technique, Ishigami *et al* [8] showed that monolayer graphene largely follows the underlying morphology of SiO_2, and they estimated the adhesion energy between graphene and SiO_2 to be $0.096\,J\,m^{-2}$, based on the interlayer van der Waals (vdW) interaction in bulk graphite. However, the measurements by Koenig *et al* [2] reported a strong adhesion of $0.45\,J\,m^{-2}$ between graphene and the SiO_2 substrate. More recently, a similar experiment yielded a considerably lower adhesion energy of $0.24\,J\,m^{-2}$ [3]. It was suggested that the difference could arise from the surface properties of SiO_2, such as surface roughness and chemical reactivity. The effect of surface roughness, which has been analysed using a macroscopic continuum model [9–11], may contribute to the experimental variations. In this paper, the influence of the surface structures and their chemical reactivity on interfacial adhesion is investigated using density functional theory (DFT).

DFT calculations of graphene on SiO_2 have been reported previously. While SiO_2 is typically amorphous in experiments, DFT calculations are generally limited to crystalline SiO_2, with only a few exceptions [12, 13]. Among the crystalline SiO_2 phases, α-quartz is the most stable under ambient conditions. Several DFT studies reported that C–O and C–Si covalent bonds can form at the graphene/SiO_2 interface due to the reactivity of dangling bonds on the SiO_2 surface [14–16]. As a result, a strong interfacial adhesion between graphene and SiO_2 was predicted. For instance, Hossain [16] calculated the adhesion energy as $62.10\,meV\,Å^{-2}$ (or equivalently,

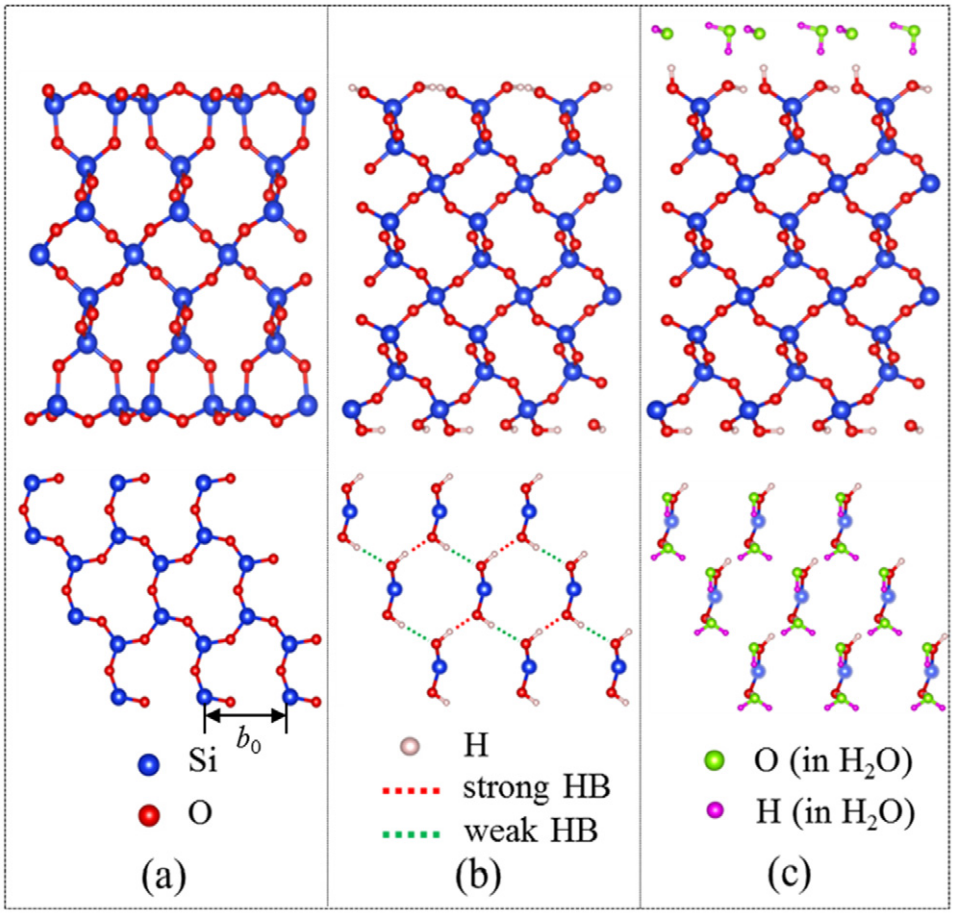

Figure 1. Side and top views of the SiO_2 substrate with different surface structures: (*a*) reconstructed, (*b*) hydroxylated and (*c*) covered by a monolayer of water molecules.

0.995 J m^{-2}) for the O-terminated SiO_2 surface. However, many experiments [2, 3, 8, 17] suggested that the interaction between graphene and SiO_2 is physisorption in nature, dominated by vdW interactions rather than covalent bonds. In fact, previous studies [18, 19] on α-quartz have shown that the cleaved (0 0 1) surface undergoes a reconstruction at around 300 K to become O-terminated with six-membered rings as shown in figure 1(*a*). Meanwhile, the under-coordinated (0 0 1) surface is hydrophilic, which commonly reacts with ambient water to yield silanol groups (Si–OH). The hydroxylated α-quartz surface is characterized by a zigzag network with alternating strong and weak hydrogen bonds as shown in figure 1(*b*). Cuong *et al* [20] studied both the reconstructed and hydroxylated α-quartz surfaces using DFT with the local density approximation (LDA). They obtained a binding energy of 14.6 meV per C atom (equivalent to an adhesion energy of 0.090 J m^{-2}) for the reconstructed surface and 12.8 meV per C atom (0.079 J m^{-2}) for the hydroxylated surface. Noticing that LDA does not take into account the dispersive interactions, Fan *et al* [21] considered vdW interactions with a semiempirical approach (DFT-D2) and obtained an adhesion energy of 0.235 J m^{-2} for the reconstructed α-quartz surface. Recently, several other methods have been proposed to account for vdW interactions in DFT calculations including approaches by Tkatchenko and Scheffler [22, 23] (vdW-TS) and Klimes *et al* [24] (optPBE-vdW). In this paper, we compare different DFT methods for interfacial adhesion between graphene and SiO_2 with different surface structures. In addition to the reconstructed and hydroxylated surfaces, water adsorption on the surface is also considered, since the silanol groups on the hydroxylated surface are sensitive to the adsorption of small molecules such as H_2O under ambient conditions. In particular, the adsorption of water on the α-quartz surface was found to be thermodynamically favourable in previous studies [25–27]. DFT calculations have shown that, when water is adsorbed on the hydroxylated surface, the weak hydrogen bonds are broken and new hydrogen bonds are formed between the hydroxyl groups and water molecules [27, 28]. When the coverage of water molecules reaches one monolayer, a hexagonal H_2O network similar to the basal plane of ice Ih is formed on the surface, as shown in figure 1(*c*).

All the DFT calculations in this study were performed using the plane-wave-based Vienna Ab-initio Simulation Package (VASP [28, 29]). Projector augmented wave (PAW [30, 31]) pseudopotentials were used to represent ionic cores, and the electronic kinetic energy cutoff for the plane-wave basis describing the valence electrons was set to 520 eV. A 4 × 4 × 1 *k*-point mesh was used for structure relaxation and a 14 × 14 × 1 *k*-point mesh for self-consistent static

Table 1. Comparison of lattice parameters for graphene and SiO_2 obtained from different DFT methods. The lattice mismatch between graphene and SiO_2 is calculated as $\varepsilon_0 = (2a_0 - b_0)/b_0$.

Method	Graphene, a_0 (Å)	SiO_2, b_0 (Å)	Lattice mismatch, ε_0 (%)
LDA	2.4462	4.8906	0.037
GGA-PBE	2.4678	5.0371	−2.02
DFT-D2	2.4685	4.9259	0.23
vdW-TS	2.4656	4.9764	−0.91
optPBE-vdW	2.4713	4.9891	−0.93
Experimental	2.4589[32]	4.9124[33]	0.11

calculation. The ground-state structural parameters of bulk SiO_2 and graphene were first calculated using the five DFT methods listed in table 1. It is found that the calculated structure is over-bound with LDA and slightly under-bound by the other methods, as compared to experiments [32, 33]. The supercell for the adhesion energy calculations consisted of a 2 × 2 graphene sheet on a 1 × 1 SiO_2 unit cell with a vacuum layer of 20 Å thickness separating the periodic images of the slab. The in-plane dimension of the supercell was set by the equilibrium lattice constant of graphene. The lattice constant of the SiO_2 substrate was adjusted by a biaxial strain to accommodate the lattice mismatch, as listed in table 1. To compute the adhesion energy, the system was fully relaxed, except for the middle layer in the SiO_2 slab, which was frozen in the bulk structure. The adhesion energy E_{ad} was then calculated by

$$E_{ad} = E_g + E_s - E_{g/s}, \quad (1)$$

where E_g, E_s and $E_{g/s}$ are energies of isolated graphene, isolated SiO_2 substrate and the graphene/SiO_2 system, respectively. It is noted that different binding positions could be obtained by shifting the relative locations between graphene and SiO_2 along the lattice vector directions, with a periodicity same as the primitive cell of graphene. As shown in figure 2(*a*), we partition the primitive cell of graphene into a 6 × 6 equal spaced mesh, so that the adhesion energy could be calculated at 36 different relative positions. The most stable configuration corresponds to the one with the lowest energy $E_{g/s}$, with which the adhesion energy is calculated.

Table 2 lists the adhesion energies from our calculations. The generalized gradient approximation with Perdew–Burke–Ernzerhof functional (GGA-PBE [34]) yields minimal adhesion for all the surface types considered, which is expected, since no vdW interactions are accounted for. It has been shown that the LDA [35] is able to predict correct interlayer distances for some layered materials including graphite. However, it is purely local and hence not able to fully describe long-range dispersion interactions. Our results indicate that LDA considerably underestimates the adhesion energy in comparison with the experimental measurements, although the predicted equilibrium separation is very close. Previous studies have shown the importance of vdW corrections to traditional DFT for describing the interfaces in graphene-based systems such as graphite [36, 37], graphene on metal substrates [38] and graphene on SiC [39]. Many schemes have been proposed for correcting

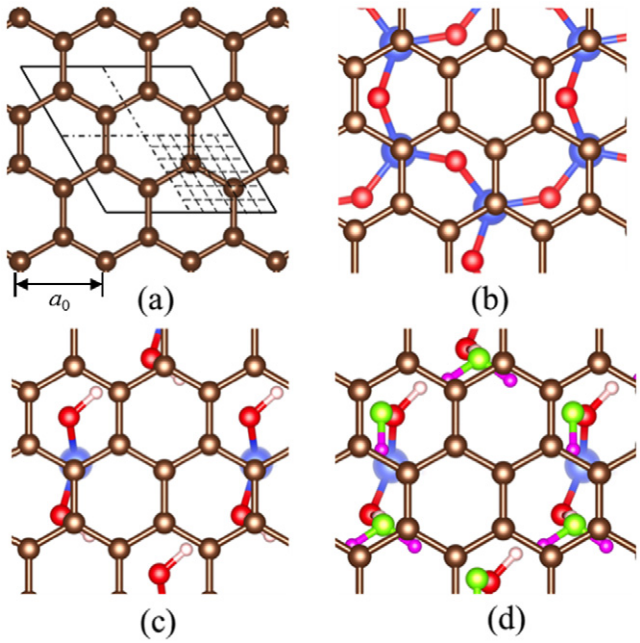

Figure 2. (*a*) Graphene lattice, with a 2 × 2 unit cell indicated by the parallelogram box, within which a primitive unit cell is partitioned into a 6 × 6 mesh. (*b*)–(*d*) Top views of the equilibrium structures for graphene on SiO_2 with different surface structures: (*b*) reconstructed, (*c*) hydroxylated and (*d*) covered by a monolayer of water molecules.

DFT calculations with dispersion effects for vdW interactions, among which the DFT-D2, vdW-TS and optPBE-vdW methods are used in the present study. The DFT-D2 method [40] adds a pairwise interatomic $C_{6AB}R_{AB}^{-6}$ term to the conventional Kohn–Sham energy, where R_{AB} is the distance between atoms A and B, and C_{6AB} is the corresponding coefficient. As shown in our results, this correction brings in appreciable adhesion energy between graphene and SiO_2. The drawback of DFT-D2 is its empirical nature, since the pairwise coefficients in the correction term are obtained by fitting, either to experiments or to post-Hartree–Fock analysis, with the requirement of being independent of the chemical environment. Tkatchenko and Scheffler proposed a more sophisticated method (vdW-TS) to compute the C_{6AB} coefficients from the mean-field ground-state electron density of molecules and solids [22, 23]. Our calculations show that the adhesion energies from vdW-TS are about 50% greater than those from DFT-D2. Another vdW corrected DFT method is optPBE-vdW [24], which uses the nonlocal correlation description from the nonempirical and electron density based Chalmers–Rutgers vdW-DF [41] method but with its exchange functional optimized based on S22 datasets [42]. It is found that the adhesion energy predicted by optPBE-vdW compares closely to the prediction by vdW-TS, and both are in good agreement with experimental measurements [2, 3].

Figures 2(*b*)–(*d*) illustrate the optimized binding structures of graphene on the three types of SiO_2 surfaces. It is noted that the most stable binding structure does not depend on the choice of DFT method. Moreover, the energy variations among the 36 binding locations are 6–10% of the total adhesion energies, indicating that the binding between

Table 2. Adhesion energy (E_{ad}) and equilibrium separation (δ_0) between graphene and SiO_2 with reconstructed, hydroxylated and water monolayer covered surfaces, obtained from different DFT methods.

	E_{ad} (J m^{-2})/δ_0 (Å)		
Method	Reconstructed	Hydroxylated	Water adsorption
GGA-PBE	0.0027/3.556	0.0055/3.420	0.0034/3.207
LDA	0.115/3.000	0.094/3.002	0.096/2.882
DFT-D2	0.229/3.006	0.166/3.043	0.134/2.800
vdW-TS	0.349/3.089	0.242/3.164	0.210/2.993
optPBE-vdW	0.311/3.069	0.258/3.036	0.224/2.883

graphene and the SiO_2 substrate is insensitive to their relative positions. It is found that the adhesion energy is reduced by surface hydroxylation and further reduced by adsorption of a water monolayer. The change of adhesion energy can be largely attributed to the change of the atomic structures of the SiO_2 surface. As can be seen in figure 1, from reconstructed to hydroxylated surface, the number density of the surface atoms (first layer of Si and O) is reduced due to reaction with H to form the H–O bonds and hydrogen bonds. Since the vdW interaction between H and C is much weaker than Si–C and O–C, the lower number density of Si and O on the hydroxylated surface leads to a lower adhesion energy compared to the reconstructed surface. With adsorption of a water monolayer, the adhesion energy includes contributions from both graphene–water and graphene–SiO_2 interactions. The graphene–water interaction was investigated previously by first-principles calculations, which calculated the adsorption energy between a water monomer and graphene to be 90 meV/H_2O [43]. With the number density of water molecules on the SiO_2 surface in our calculation (9.33 nm^{-2}), the graphene–water interaction would contribute 0.134 J m^{-2} towards the total adhesion energy of 0.210 J m^{-2}. The contribution from the graphene–SiO_2 interaction is then 0.076 J m^{-2}, which is much lower than the adhesion energy between graphene and a bare SiO_2. The presence of the water monolayer thus weakens the vdW interaction between graphene and SiO_2, which may be partly attributed to the relatively large separation between graphene and SiO_2 (5.06 Å). While the full hydroxylation and monolayer water coverage of the surface are considered here, the density of silanol groups or water adsorption for a real SiO_2 surface would depend on the ambient conditions, such as the relative humidity. Nevertheless, our study suggests that changes in the surface structure due to chemical reactivity of the SiO_2 surface with water may contribute to the variation of adhesion energies measured in experiment [2, 3], in addition to the macroscopic effects due to surface roughness. We note that the macroscopic capillary effect is not considered in this study, which may become important at relatively high humidity and give rise to different characteristics of adhesion [25].

In all cases, it is found that graphene maintains its planar configuration on top of the SiO_2 substrate. This is expected for two reasons: the substrate surface is atomically smooth (i.e. no macroscopic roughness is considered) and no temperature effect is taken into account in the DFT calculations (hence no thermal rippling). As a result, the separation (δ) between graphene and the substrate can be defined as the distance

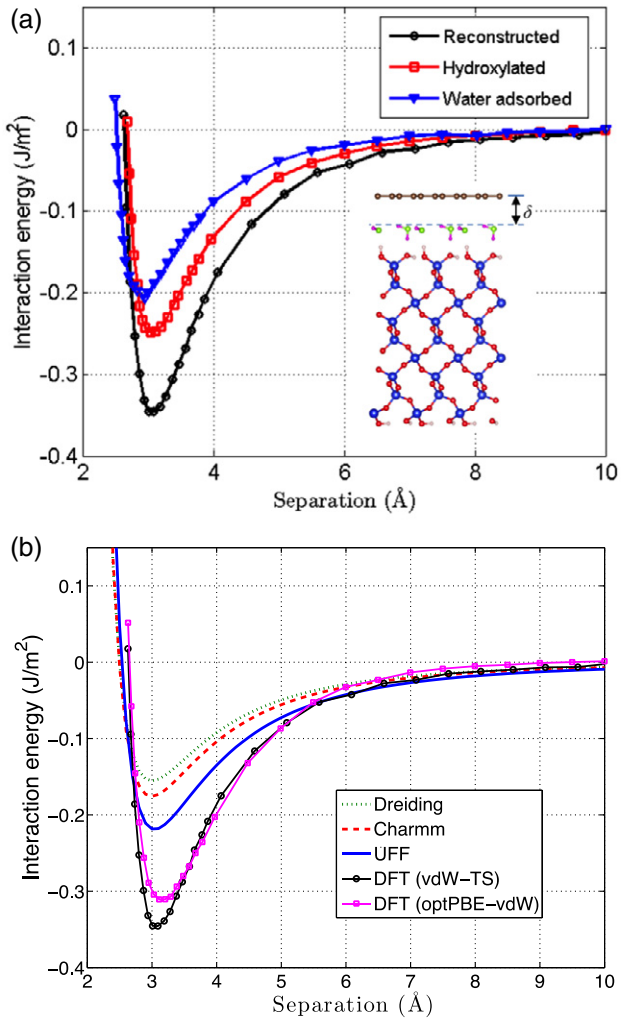

Figure 3. (a) Interaction energy as a function of separation between graphene and SiO_2, calculated with the vdW-TS method for three surface structures. The inset shows the side view of graphene on SiO_2 with a water monolayer. (b) Comparison of the interaction energy calculated from DFT (vdW-TS and optPBE-vdW) and three empirical force fields for graphene on a reconstructed SiO_2 surface.

between the C atoms in graphene and the topmost atoms of the substrate (including water molecules) as shown in figure 3(a). By freezing the out-of-plane displacement of graphene, the interaction energy U can be calculated at different separations; the minimum interaction energy is reached at the equilibrium separation (δ_0). The function $U(\delta)$, calculated using the vdW-TS method, is plotted in figure 3(a) for three different surface structures. In all three cases, the interaction energy functions show long-range tails, revealing the nature of dispersion interactions. As a simple mathematical model, the Lennard-Jones (LJ) potential is commonly used in atomistic simulations based on empirical force fields to account for the dispersion forces, including the graphene/SiO_2 interface [44, 45]. The LJ potential between atoms i and j can be written as

$$V_{ij}(R_{ij}) = \varepsilon_{ij}\left[\left(\frac{\sigma_{ij}}{R_{ij}}\right)^{12} - \left(\frac{\sigma_{ij}}{R_{ij}}\right)^{6}\right], \qquad (2)$$

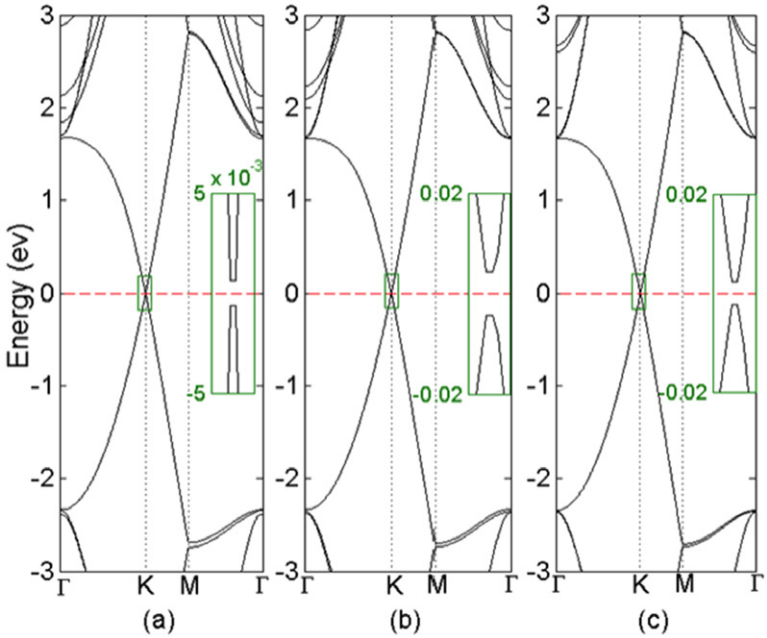

Figure 4. Electronic band structures of graphene on SiO_2 with different surface structures: (*a*) reconstructed, (*b*) hydroxylated and (*c*) covered by a monolayer of water molecules. The insets show the band gap around the K point.

where R_{ij} is the atomic distance, σ_{ij} and ε_{ij} are the pairwise parameters. By integrating equation (2) with respect to all atoms, the interaction energy between graphene and SiO_2 substrate per unit area can be obtained as [9]

$$U_{\mathrm{LJ}}(\delta) = \sum_j \frac{2\pi\rho_j\varepsilon_{ij}}{A_0}\left(\frac{\sigma_{ij}^{12}}{45\delta^9} - \frac{\sigma_{ij}^{6}}{6\delta^3}\right), \qquad (3)$$

where the subscript i represents a C atom, j represents Si or O, ρ_j is the number density of Si or O atoms in the substrate ($\rho_{\mathrm{Si}} = 25.0\,\mathrm{nm}^{-3}$ and $\rho_{\mathrm{O}} = 50.0\,\mathrm{nm}^{-3}$), and A_0 is the area of a unit cell of graphene. The summation in equation (3) takes both Si–C and O–C interactions into account. In the empirical force field, the parameters σ_{ij} and ε_{ij} for each pairwise interaction are obtained by fitting to experiments or first-principles calculations. Considering three typical force fields (UFF [46], Charmm [47] and Dreiding [48]), we calculated the interaction energy $U_{\mathrm{LJ}}(\delta)$ using equation (3) for the reconstructed SiO_2 surface, as shown in figure 3(*b*). Apparently, the equilibrium separation between graphene and SiO_2 is close to the DFT result, but the adhesion energy is underestimated by the empirical methods. For the hydroxylated and water monolayer covered SiO_2 surfaces, the use of empirical force fields would be more problematic. In practice, more sophisticated force fields with delicate parametrization could yield more accurate results. The present results from the vdW corrected DFT calculations could provide guidance for selecting appropriate force fields to study the graphene/SiO_2 interface.

To further investigate the interfacial interaction and its potential impact on the physical properties of graphene, we calculated the electronic structures of the graphene/SiO_2 system. The band structures obtained from the vdW-TS method are shown in figure 4. The shape of the Dirac cone of the pristine monolayer graphene is preserved for all three surfaces with tiny band gaps at the K point. The band gap opening can be understood by the breaking of the sublattice symmetry of graphene due to its interaction with the substrate. Such a mechanism has a more significant effect on band gap opening of graphene on SiC [49] and hexagonal boron nitride [50] substrates, but the effect is negligible for the graphene/SiO_2 system since the band gap is much less than the thermal energy at room temperature (~25 meV). Moreover, it is noted that there is no Fermi level shift in the three systems, indicating no significant charge transfer induced electrostatic interactions. Previous experiments [51, 52] have shown some evidence for both p-type and n-type doping of graphene on SiO_2 substrates, which may be accounted for by including non-ideal aspects of the system such as surface defects and other environmental effects. Based on an analytical model, Sabio *et al* [53] studied electrostatic interactions between graphene and SiO_2 along with other materials (including water molecules) in its environment. They found that the leading electrostatic interactions arise from the surface polar modes of SiO_2 and electrical dipoles of water molecules, with estimated interaction energies of 0.4 meV Å^{-2} (0.0064 J m^{-2}) and 1 meV Å^{-2} (0.016 J m^{-2}), respectively; both are significantly lower than the adhesion energies due to the vdW interactions in the present DFT calculations.

In conclusion, the interfacial adhesion between graphene and SiO_2 substrate is studied by DFT methods with vdW interactions. It is found that the interaction between graphene and SiO_2 is dominated by dispersion forces. The adhesion energy is reduced by surface hydroxylation and further reduced by adsorption of water molecules. Among the DFT methods considered in the present study, we suggest that the vdW-TS and optPBE-vdW methods are both suitable for studying the interactions between graphene and SiO_2. Moreover, the discrepancy between DFT and empirical force fields suggests a need for more sophisticated force fields to describe the graphene/SiO_2 system. Finally, it is found that the vdW

interactions have negligible influence on the electronic band structure of graphene.

Acknowledgments

The authors gratefully acknowledge financial support of this work by the National Science Foundation through Grant No CMMI-1130261. The authors acknowledge the Texas Advanced Computing Center (TACC) at the University of Texas at Austin for providing HPC resources that have contributed to the research results reported within this paper.

References

[1] Wu Y Q, Farmer D B, Xia F N and Avouris P 2013 *Proc. IEEE* **101** 1620
[2] Koenig S P, Boddeti N G, Dunn M L and Bunch J S 2011 *Nature Nanotechnol.* **6** 543
[3] Boddeti N G, Koenig S P, Long R, Xiao J L, Bunch J S and Dunn M L 2013 *J. Appl. Mech.* **80** 040909
[4] Zong Z, Chen C L, Dokmeci M R and Wan K T 2010 *J. Appl. Phys.* **107** 026104
[5] Yoon T, Shin W C, Kim T Y, Mun J H, Kim T S and Cho B J 2012 *Nano Lett.* **12** 1448
[6] Cao Z, Wang P, Gao W, Tao L, Suk J W, Ruoff R S, Akinwande D, Huang R and Liechti K M 2014 *Carbon* **69** 390
[7] Novoselov K S, Geim A K, Morozov S V, Jiang D, Zhang Y, Dubonos S V, Grigorieva I V and Firsov A A 2004 *Science* **306** 666
[8] Ishigami M, Chen J H, Cullen W G, Fuhrer M S and Williams E D 2007 *Nano Lett.* **7** 1643
[9] Aitken Z H and Huang R 2010 *J. Appl. Phys.* **107** 123531
[10] Gao W and Huang R 2011 *J. Phys. D: Appl. Phys.* **44** 452001
[11] Li T and Zhang Z 2010 *J. Phys. D: Appl. Phys.* **43** 075303
[12] Miwa R H, Schmidt T M, Scopel W L and Fazzio A 2011 *Appl. Phys. Lett.* **99** 163108
[13] Rudenko A N, Keil F J, Katsnelson M I and Lichtenstein A I 2011 *Phys. Rev.* B **84** 085438
[14] Kang Y J, Kang J and Chang K J 2008 *Phys. Rev.* B **78** 115404
[15] Shemella P and Nayak S K 2009 *Appl. Phys. Lett.* **94** 032101
[16] Hossain M Z 2009 *Appl. Phys. Lett.* **95** 143125
[17] Stolyarova E, Rim K T, Ryu S M, Maultzsch J, Kim P, Brus L E, Heinz T F, Hybertsen M S and Flynn G W 2007 *Proc. Natl Acad. Sci. USA* **104** 9209
[18] Rignanese G M, De Vita A, Charlier J C, Gonze X and Car R 2000 *Phys. Rev.* B **61** 13250
[19] Goumans T P M, Wander A, Brown W A and Catlow C R A 2007 *Phys. Chem. Chem. Phys.* **9** 2146
[20] Cuong N T, Otani M and Okada S 2011 *Phys. Rev. Lett.* **106** 106801
[21] Fan X F, Zheng W T, Chihaia V, Shen Z X and Kuo J L 2012 *J. Phys.: Condens. Matter* **24** 305004
[22] Bucko T, Lebegue S, Hafner J and Angyan J G 2013 *Phys. Rev.* B **87** 064110
[23] Tkatchenko A and Scheffler M 2009 *Phys. Rev. Lett.* **102** 073005
[24] Klimes J, Bowler D R and Michaelides A 2010 *J. Phys.: Condens. Matter* **22** 022201
[25] Adamson A W and Gast A P 1990 *Physical Chemistry of Surfaces* (New York: Wiley)
[26] Chen Y W and Cheng H P 2010 *Appl. Phys. Lett.* **97** 161909
[27] Yang J J and Wang E G 2006 *Phys. Rev.* B **73** 035406
[28] Kresse G and Furthmuller J 1996 *Phys. Rev.* B **54** 11169
[29] Kresse G and Hafner J 1993 *Phys. Rev.* B **47** 558
[30] Kresse G and Joubert D 1999 *Phys. Rev.* B **59** 1758
[31] Blochl P E 1994 *Phys. Rev.* B **50** 17953
[32] Baskin Y and Meyer L 1955 *Phys. Rev.* **100** 544
[33] Will G, Bellotto M, Parrish W and Hart M 1988 *J. Appl. Crystallogr.* **21** 182
[34] Perdew J P, Burke K and Ernzerhof M 1996 *Phys. Rev. Lett.* **77** 3865
[35] Perdew J P and Zunger A 1981 *Phys. Rev.* B **23** 5048
[36] Rydberg H, Dion M, Jacobson N, Schroder E, Hyldgaard P, Simak S I, Langreth D C and Lundqvist B I 2003 *Phys. Rev. Lett.* **91** 126402
[37] Lundqvist B I *et al* 2011 *Surf. Sci.* **493** 253
[38] Vanin M, Mortensen J J, Kelkkanen A K, Garcia-Lastra J M, Thygesen K S and Jacobsen K W 2010 *Phys. Rev.* B **81** 081408
[39] Nemec L, Blum V, Rinke P and Scheffler M 2013 *Phys. Rev. Lett.* **111** 065502
[40] Grimme S 2006 *J. Comput. Chem.* **27** 1787
[41] Dion M, Rydberg H, Schroder E, Langreth D C and Lundqvist B I 2004 *Phys. Rev. Lett.* **92** 246401
[42] Jurecka P, Sponer J, Cerny J and Hobza P 2006 *Phys. Chem. Chem. Phys.* **8** 1985
[43] Ma J, Michaelides A, Alfe D, Schimka L, Kresse G and Wang E G 2011 *Phys. Rev.* B **84** 033402
[44] Bellido E P and Seminario J M 2010 *J. Phys. Chem.* C **114** 22472
[45] Paek E and Hwang G S 2013 *J. Appl. Phys.* **113** 164901
[46] Rappe A K, Casewit C J, Colwell K S, Goddard W A and Skiff W M 1992 *J. Am. Chem. Soc.* **114** 10024
[47] Cruz-Chu E R, Aksimentiev A and Schulten K 2006 *J. Phys. Chem.* B **110** 21497
[48] Mayo S L, Olafson B D and Goddard W A 1990 *J. Phys. Chem.* **94** 8897
[49] Zhou S Y, Gweon G H, Fedorov A V, First P N, De Heer W A, Lee D H, Guinea F, Neto A H C and Lanzara A 2007 *Nature Mater.* **6** 770
[50] Giovannetti G, Khomyakov P A, Brocks G, Kelly P J and van den Brink J 2007 *Phys. Rev.* B **76** 073103
[51] Romero H E, Shen N, Joshi P, Gutierrez H R, Tadigadapa S A, Sofo J O and Eklund P C 2008 *ACS Nano* **2** 2037
[52] Ryu S, Liu L, Berciaud S, Yu Y J, Liu H T, Kim P, Flynn G W and Brus L E 2010 *Nano Lett.* **10** 4944
[53] Sabio J, Seoanez C, Fratini S, Guinea F, Castro A H and Sols F 2008 *Phys. Rev.* B **77** 195409